

Investigation of the Attachment of Circulating Endothelial Cells to a Cell Probe: Combined Experimental and Numerical Study

Felix Hehnen,* Gabi Wendt, Jens Schaller, Paul Geus, Joachim Villwock, Ulrich Kertzsch, and Leonid Goubergrits

Circulating endothelial cells (CECs) are a reliable biomarker for cardiovascular diseases (CVDs). A major unresolved challenge limiting the widespread use of CECs for the diagnosis and monitoring of CVDs is their unreliable detection. This problem is mainly attributed to the low sample volume (5–10 mL) of commonly used *ex vivo* CEC isolation methods. To overcome this limitation, the BMProbe for the *in vivo* isolation of CECs is proposed. It consists of a twisted medical flat wire with a polymer-coated surface functionalized with anti-CD105 antibodies. A combined experimental and numerical study is performed to investigate which flow conditions lead to an increased cell attachment to the probe's surface. Endothelial cells are solved in a dextran solution and circulated in a flow system containing the BMProbes. Microscopic images of the attached CECs are taken. In addition, the experiments are simulated using a computational fluid dynamics (CFD) flow solver to quantify the flow conditions at the probe's surface. The microscopic images are superimposed with the CFD data to investigate the influence of wall shear rate and wall normal rate on the attachment of CECs to the probe. Most of all attached cells (85.5%) are found in areas of negative wall normal rate.

1. Introduction

Cardiovascular diseases (CVDs) are by far the most common cause of death and disability. They cause an estimated 27% of all global deaths.^[1] With an aging population, these numbers will rise. Many of these deaths could be prevented if there were reliable biomarker to predict fatal cardiovascular events for high-risk patients. But many of these events involve sudden atherosclerotic plaque rupture and therefore remain highly unpredictable. Recent research has identified circulating endothelial cells (CECs) as a reliable biomarker for cardiovascular events.^[2–4] Endothelial cells are lining the inner surface of blood vessels and regulate the interaction between blood and vessel wall. Cardiovascular events often result in an endothelial damage associated with a release of endothelial cells into the bloodstream, which are further known as

CECs.^[5] The concentration of CECs in blood seems to correlate with the severity of the present CVD and can therefore be used as a diagnostic and prognostic biomarker as well as for posttreatment monitoring.^[3,5] However, the concentration of CECs in blood from patients with CVDs such as heart failure with preserved or reduced ejection fraction or with arterial hypertension is very low and only reaches ≈ 60 out of 5 billion blood cells in 1 mL of blood.^[3] Liquid biopsies are becoming increasingly popular for isolating rare cells (e.g., endothelial or tumor cells) from blood.

Different approaches were proposed to isolate and analyze circulating rare cells. Some techniques such as fluorescence-activated cell sorting and immunomagnetic isolation have been established for years.^[6] Recently more and more size-based isolation methods have been developed. These methods include microfluidic sorting devices and membrane microfilters.^[7] All mentioned techniques are *in vitro* tests based on a blood sample.


The current study is based on an alternative liquid biopsy approach using a wire-based cell probe with a functionalized surface to isolate CECs. This cell probe, called the BMProbe, from the company Invicol is a relatively new method to isolate CECs *in vivo*. A similar method is already known to isolate circulating tumor cells (CTCs) *in vivo*.^[8,9] It is inserted into the patient's cubital vein using a standard peripheral venous catheter. The

F. Hehnen, J. Schaller, P. Geus, U. Kertzsch, L. Goubergrits
Institute of Computer-Assisted Cardiovascular Medicine
Charité – Universitätsmedizin Berlin
13353 Berlin, Germany
E-mail: felix.hehnen@charite.de

G. Wendt, P. Geus
INVICOL GmbH
13353 Berlin, Germany

J. Villwock
Institute of Mechanical Engineering
Beuth Hochschule für Technik Berlin
University of Applied Sciences
13353 Berlin, Germany

L. Goubergrits
Cardiovascular Modelling and Simulation
Einstein Center Digital Future
10117 Berlin, Germany

 The ORCID identification number(s) for the author(s) of this article can be found under <https://doi.org/10.1002/adem.202101317>.

© 2021 The Authors. Advanced Engineering Materials published by Wiley-VCH GmbH. This is an open access article under the terms of the Creative Commons Attribution-NonCommercial License, which permits use, distribution and reproduction in any medium, provided the original work is properly cited and is not used for commercial purposes.

DOI: 10.1002/adem.202101317

surface of the probe is coated with a biocompatible polymer and functionalized with anti-CD105 antibodies, so that only CECs can adhere to it. After 30 min, the probe is removed from the vein, the cells are fixed and stained, and the number of attached CECs can be counted and used for downstream analysis.

While other liquid biopsy methods of isolating rare cells such as CellSearch are limited to a small amount of blood drawn from the patient,^[10] the BMProbe's diagnosis is based on the screening of a much larger blood volume. The number of rare cells potentially available for the diagnostic procedure would therefore be much higher. If relatively large number of CECs are available, an additional biomolecular analysis or mRNA analysis can be done. However, it has not been conclusively clarified how large the screened volume of the probe actually is. Various studies came up with very different values ranging from a few mL^[11,12] up to more than a liter.^[9] However, it should be noted that the data collected so far are studies of the CellCollector of the company Gilupi. The BMProbe used in this study varies from the CellCollector in terms of shape and coating process.

The two factors—the shape and the functional coating of the BMProbe—are crucial for the number of CECs that the probe can isolate from the blood. The probe's shape affects the near-wall flow field, which in turn affects the near-wall cell movement. This flow is of key interest because only near-wall cells can interact with the probe's surface. It is known that a laminar flow along a flat surface with a distinct boundary layer provides only a very low contact probability for the particles and the surface. As there is practically no vertical movement in this flow, the transport of the cells toward the wall is only possible by diffusion.^[13] Therefore, it is necessary to use a probe geometry that interrupts the laminar flow profile along the surface of the probe and creates a strong convection in the near-wall flow. A study^[11] concluded that the geometry of the twisted flat wire used in this study leads to increased cross-flow and thus improved contact between cells and surface of the probe. The influence of near-wall flow has also been studied for the attachment of platelets to surfaces.^[14,15] It was found that attachment can be regarded as a function of convection and diffusion near the wall.^[16] The convection can be divided into a tangential and a normal velocity component. Diffusion, which is not affected by the flow, is additionally responsible for a sudden movement of a cell toward the surface.

Based on this knowledge, this study investigated the near-wall flow along the BMProbe in order to quantify hemodynamic parameters advantageous for the deposition of CECs. For this purpose, a combined experimental and numerical study was carried out, in which the attachment of CECs to the probe was analyzed under different flow conditions.

2. Study Design

This study combines an experimental in vitro study with a computational modeling approach. Human umbilical vein endothelial cells (HUVECs) were diluted in a dextran solution, which is supposed to mimic the non-Newtonian flow properties of blood. This suspension circulates in a specially designed test circuit, allowing a simultaneous testing of several BMProbes under controlled flow conditions. The experiment is repeated for four different mean flow velocities. In vitro tests are followed by a microscopic analysis of the CECs isolated by the probe, including cell counting and an

assessment of the exact cell attachment position on the probe. Finally, the flow along the probe is simulated with a computational fluid dynamics (CFD) flow solver. The accurately determined flow parameters along the probe are correlated with cell depositions determined by the experiments, in order to find flow conditions promoting cells adhesion to the probe's surface.

2.1. Flow Parameter

To investigate the impact of the near-wall flow on the deposition of CECs to the surface of the probe, flow parameters were selected to characterize tangential and vertical near-wall fluid movement. For tangential or parallel wall movement, the wall shear rate (WSR)

$$\text{WSR} = \left(\frac{\partial v_{\parallel}}{\partial x_{\perp}} \right)_{\text{wall}} \quad (1)$$

was used. This item is directly linked with the wall shear stress (WSS) by the dynamic viscosity. For vertical wall movement, a similar parameter—wall normal rate (WNR)—was designed

$$\text{WNR} = \left(\frac{\partial v_{\perp}}{\partial x_{\perp}} \right)_{\text{wall}} \quad (2)$$

where v_{\parallel} denotes the velocity component parallel to the wall and v_{\perp} the velocity component normal to the wall. Correspondingly, x_{\perp} denotes the length unit that is normal to the wall. With a negative WNR, the flow is directed toward the wall, with a positive WNR the flow direction points away from the wall.

3. Results

3.1. Experimental Results

In the experimental part of this study, HUVECs are isolated with the BMProbe from an in vitro circulation model (Figure 5). The attached CECs are evaluated under the microscope (Figure 4b). To understand which near-wall flow promotes cell attachment to the probe, it is necessary to record the exact position of each cell on the probe. In this way, the associated flow data from the CFD simulation can be assigned to each attached cell. Each microscope image captures exactly one winding of the probe (Figure 4b). **Table 1** lists all images evaluated for the four mean inflow velocities 1, 2, 3, and 5 cm s⁻¹. In total, 236 images with 2094 bound CECs were evaluated.

Table 1. The experimental studies were performed with four different incident flow velocities: 1, 2, 3, and 5 cm s⁻¹. For each velocity, ten BMProbes were evaluated. As not all microscope images are suitable for automatic image evaluation, the number of images evaluated for the four velocities varies.

Mean inflow velocity [cm s ⁻¹]	Number of images	Number of bound cells	Cells per image
1	60	477	7.95
2	58	562	9.69
3	54	520	9.63
5	64	535	8.36

The number of attached cells for the four different inflow velocities is shown in **Figure 1**. Each evaluated microscope image (i.e., each winding of the cell probe) is considered as one experiment. With the help of a CFD simulation, it could be shown that the flow conditions are the same for each of the considered windings. The Kruskal–Wallis test reveals that the four groups are statistically significantly different from each other ($p = 0.0077$). However, it should be noted that only the 1 cm s^{-1} group is significantly different from the 2 cm s^{-1} ($p = 0.021$) and the

3 cm s^{-1} ($p = 0.0352$) group. No significant differences can be demonstrated for all other groups.

Thus, a relationship cannot be clearly found between the velocity of the parent flow and the total number of cells attached.

3.2. Combined Experimental and Numerical Results

In order to investigate the relationship between the near-wall flow and the accumulation of cells on the wall, the regional distribution of the accumulated cells on the probe is examined in more detail. In **Figure 2**, all attached cells are merged into one image for the velocities 1 and 5 cm s^{-1} and superimposed with the CFD data. The CFD data of the WNR (Figure 2a,b) and the WSR (Figure 2c,d) are presented. As can be seen in Figure 2, the cells mostly attach along the upper edge of the probe. This is the edge facing the flow. The same pattern is also found in the experiments with 2 and 3 cm s^{-1} . The CFD data seem to confirm that a high number of cells accumulate in the areas where the WNR is directed toward the wall (see red colored areas in Figure 2a,b).

In **Figure 3**, each attached cell is mapped to its respective value of WNR and WSR. If the value of the WNR is negative, the flow points toward the wall; if the value is positive, the flow points away from the wall. 1790 of 2094 attached cells are found in areas of negative WNR. This corresponds to 85.5% of all attached cells. The WSR on the surface of the probe increases linearly with the main inflow velocity. However, the pattern of cell attachment to the probe seen in Figure 2 does not seem to be affected by different tangential flows on the wall of the probe.

The results of the combined numerical and experimental study show that the CECs predominantly attach in areas with negative WNR in a small range of the WNR between -0.5 and 0.0 s^{-1} as well as relatively low WSR below 150 cm s^{-1} .

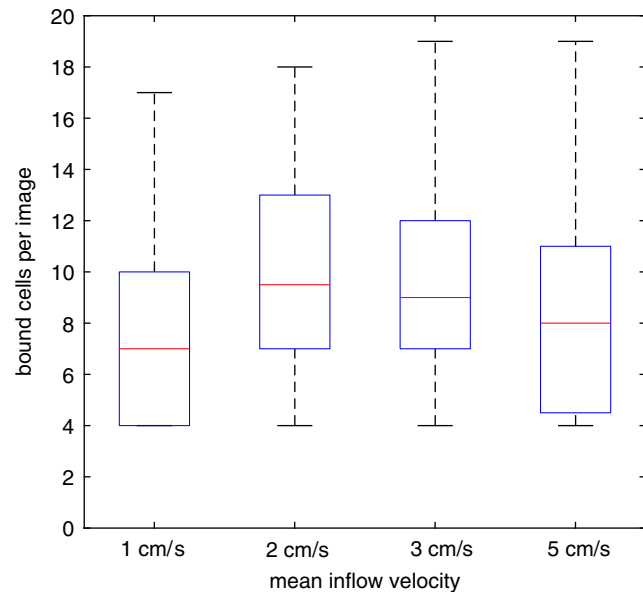


Figure 1. Experiments were made with four different mean inflow velocities. The number of evaluated images and cells per velocity is shown in Table 1 and visualized in this boxplot. On each box, the central mark indicates the median, and the bottom and top edges of the box indicate the 25th and 75th percentiles, respectively. The whiskers extend to the most extreme data points. Statistically significant differences for the four groups can only be found between the velocities 1 and 2 cm s^{-1} ($p = 0.021$), and 1 and 3 cm s^{-1} ($p = 0.0352$).

4. Discussion

In order to use the BMProbe as a reliable diagnostic tool, it is essential that it is able to bind as many CECs as possible from

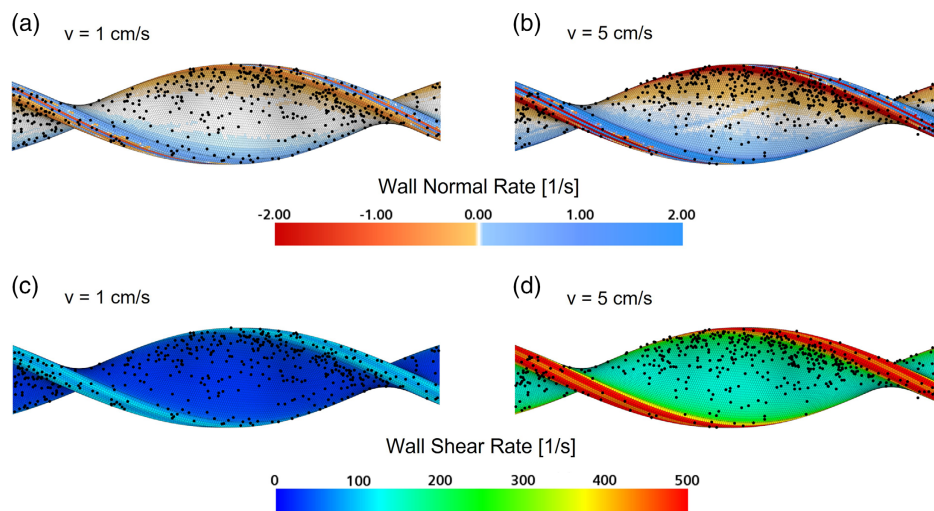


Figure 2. Combined representation of CFD results for the simulated WNR and WSR distributions together with in vitro CEC depositions marked by black dots. Exemplary results for two investigated conditions are represented: mean inlet velocities of 1 and 5 cm s^{-1} .

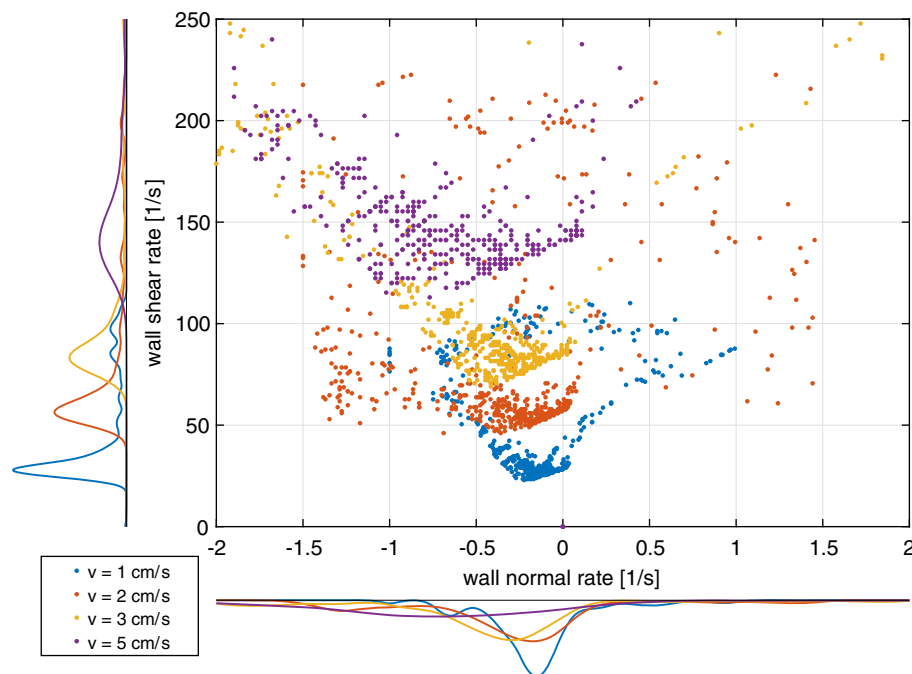


Figure 3. This scatter plot shows every single assessed cell that has attached to the surface of the BMProbe, evaluated according to the tangential and normal flow components of the near-wall flow. Of the total of 2094 cells, 1790 cells (85.5%) accumulated under a negative WNR. This means that the flow direction of the near-wall flow is directed toward the wall. The WSR at which the cells accumulate depends strongly on the main inflow velocity. It should be noted that the WSR is about 100 times higher than the WNR.

the passing blood. For this, the convection in the near-wall flow must be increased and the laminar flow along the surface must be disturbed.^[17] This is ensured by the twisted geometry of the probe, which functions as a passive mixing structure.^[11] To further investigate the fluid mechanical conditions leading to the attachment of cells to the BMProbe and to find a flow parameter to describe the ability of the probe to isolate cells from the flow, a combined experimental and numerical study was done.

In vitro tests assessed CEC attachment to the functionalized surface of the BMProbe, which cannot be simulated without additional extended tests of cell attachment. CFD analysis, on the other hand, provides an accurate assessment of the near-wall flow field. Evaluating the flow field near the complex shape of the probe using any optical flow visualization methods such as particle image velocimetry or laser Doppler anemometry is challenging due to the optical access and light reflections from the cell probe. However, by combining the numerical and experimental methods, all the necessary information could be collected with minimal effort. Due to the simple geometry of the test section and the low flow velocities, it can be assumed that the numerical simulations of the flow around the probe provide correct values. As no influence of accumulated cells on the accumulation of further cells is known, and also the attachment of cells does not significantly change the geometry of the probe, it is reasonable that cell attachment is not modeled in the CFD simulation. Note that the complex shape of the wire makes any in situ measurements using optical methods challenging. For these reasons, a numerical simulation of the flow seems to be sufficient and makes further in situ measurements of the flow with CEC deposition in the test section unnecessary.

The results of the study show that the normal component of the near-wall convective flow has a considerable effect on the attachment of cells. The majority of all attached cells (85.5%) were found in areas with a negative normal flow. The used parameter “wall normal rate” seems to be useful to identify the areas where cell attachment is likely (Figure 2). However, the orientation of the normal flow seems to be of much more importance than its magnitude.

In contrast, an influence of the WSR cannot be determined with certainty. The results of the CEC deposition experiments show in Figure 2 that deposition correlates with low WSRs. The deposition peaks tended to decrease with higher WSRs. However, these results also correlate with increasing inlet flow rates that shift the minimum WSR values toward higher values. Accordingly, this finding should be taken with caution. That shear flow can have an effect on cell–surface interaction is known for other cells from the blood circulation, e.g., platelets.^[16] However, an influence of the WNR on the deposition of CECs on the functional surface of the probe cannot be completely ruled out with this study.

In addition to flow conditions, the functionalized surface of the BMProbe itself also has an effect on CEC deposition. The investigation of the functionalized surface was beyond the scope of this study. However, the quality of the functionalized surface coating was continuously monitored.

The current study has some limitations. The in vitro tests were performed under steady-state flow conditions, which neglected pulsatile flow. To discuss the influence of pulsatile flow, it should be noted that the flow rate pulsatility is much lower in veins compared to arteries. The mean ratio of peak to mean flow rate in a

cephalic vein, 1.36, is significantly smaller than the mean ratio of 3.84 in a brachial artery.^[18] In this study, experiments were performed with an mean flow velocity between 1 and 5 cm s⁻¹, corresponding to a ratio of 5. No significant differences in the number of attached cells could be detected. Therefore, it can be assumed that pulsatility is not likely to have a major influence.

Dextran solution was used instead of blood. Dextran solution mimics the non-Newtonian behavior of blood, but it is not a cell suspension like blood. Blood cells, and especially erythrocytes, could affect the near-wall transport of CECs and thus the adhesion of CECs to the probe. For example, the influence of erythrocytes on local diffusivity of blood is known from experiments on platelet deposition.^[19] As in this study the influence of a convective transport on the accumulation of CECs is considered, the diffusivity of the test fluid plays a negligible role and will not significantly affect the results of this study.

The in vitro test chamber was designed with a BMProbe placed in the center of the test section parallel to the flow. This design resulting in the same flow condition for each winding segment of the probe allowed a better statistical evaluation of experiments with a smaller number of tests. In human applications, the BMProbe is inserted into the vein at an angle, resulting in a more complex and variable flow conditions along the probe length. These different flow conditions are largely covered in our experiments due to the different mean flow velocities at which the experiments were conducted. However, a more realistic position of the probe should be investigated in future tests. All results of the current study are valid for CECs. In order to use the gained knowledge also for methods to isolate CTCs, the abovementioned study should be repeated with CTCs.

5. Conclusion

A combined experimental and numerical study was elaborated to investigate cell deposition on the functionalized surface of a BMProbe under flow conditions. Based on the results of experiments and flow simulations, a map of attached cells was defined as a function of two hemodynamic parameters describing the near-wall flow—the WSR and the WNR. This map allows an estimation of cell attachment to a surface of any simulated cell probe

design without time-consuming and expensive in vitro testing. It can be used to accelerate the development of new optimized cell probes.

6. Experimental Section

The BMProbe: The BMProbe consists of an ≈160 mm-long medical stainless steel flat wire. It has a width of 0.8 mm and a thickness of 0.15 mm. The probe's edges are rounded (Figure 4a) to avoid damaging the blood vessel's inner wall. The first 40 mm of each wire was twisted with an in-house twisting device. The twisted part of the wire forms the base of the functional surface. It is coated with a photoactive polymer to which any immunoglobulin G antibody can be applied to. To isolate CECs, the BMProbe is coated with the anti-CD105 antibody. CD105 is a proliferation-associated and hypoxia-inducible protein, abundantly expressed on angiogenic endothelial cells. The anti-CD105 antibodies for the characterization of CECs have been published in several publications.^[20,21] Compared to anti-CD146, anti-CD105 had a lower binding of unspecific cells. The binding properties were determined in in vitro experiments using healthy donor blood. These and other studies that led to the development of the BMProbe will not be discussed in detail, as this publication mainly focuses on the cell attachment process caused by the near-wall flow and not on the antigen–antibody interaction.

Experimental Study: In the experiments, the probes were placed in a test stand circuit filled with cell suspension. A schematic sketch of the used test circuit is shown in Figure 5. It consists of six test sections (marked with the red dashed box in Figure 5) connected in series, a roller pump and a reservoir with the cell suspension. Six test sections allow to simultaneously investigate the CEC deposition on six probes. The cell probes are inserted into the test sections and the cell suspension flows around them. For the experiments, two flow systems were used in parallel for each of the four different inflow velocities. In this way, 12 cell probes could be evaluated for each inflow velocity. Ten of these were provided with the antibody coating and two were uncoated as zero samples in the system.

The test section consists of a 113.5 mm-long PU tube. The inner diameter is 2 mm at the inlet and outlet and up to 4 mm in the middle of the tube (Figure 6a). At each end of the tube there is a three-way stopcock to which the next test section can be attached (Figure 6b). Furthermore, the BMProbe is inserted into the system through the inlet of the three-way stopcock.

Before the probe is inserted, the flow system is blocked with a 3% BSA/PBS solution for 30 min. The system is then filled with fresh cell suspension and the cell probes are inserted into the flow system. The cell suspension consists of a 10% dextran solution to which HUVECs are added. HUVECs are endothelial cells from the vein of an umbilical cord. They are easily available, inexpensive, and therefore often used for endothelial cell studies.^[22] After preparing the 10% dextran solution, the HUVECs are prepared, counted, and added to the dextran solution

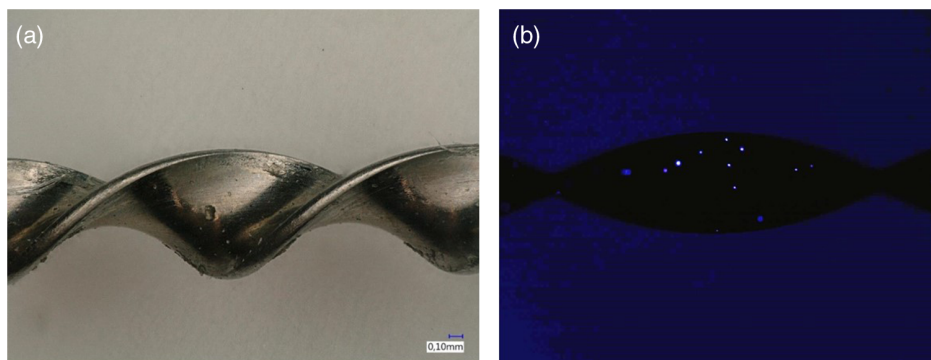


Figure 4. a) The functional front part of the cell probe consists of a twisted flat wire. The edges of the wire are rounded to avoid damaging the vessel wall. The twisted surface is coated with a polymer to which the anti-CD105 antibody is applied. b) Under the fluorescence microscope, the Hoechst-stained cells that have adhered to the probe can be detected.

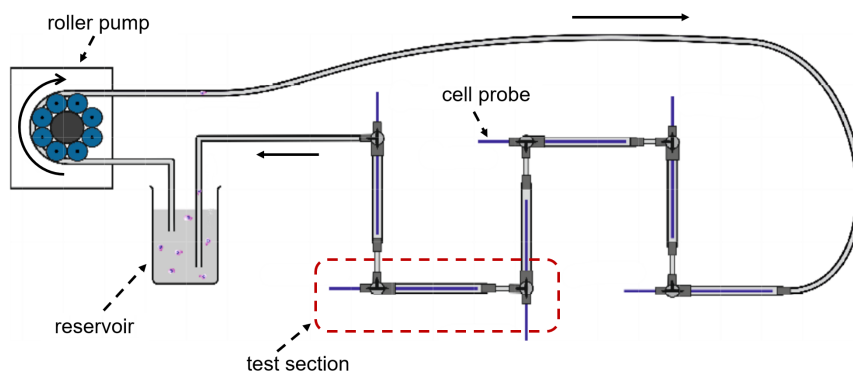


Figure 5. Schematic sketch of the flow system for the in vitro isolation of CECs, consisting of six test sections. A cell probe is placed in a fixed position in each test section. A roller pump pumps the cell suspension from a reservoir through the flow system.

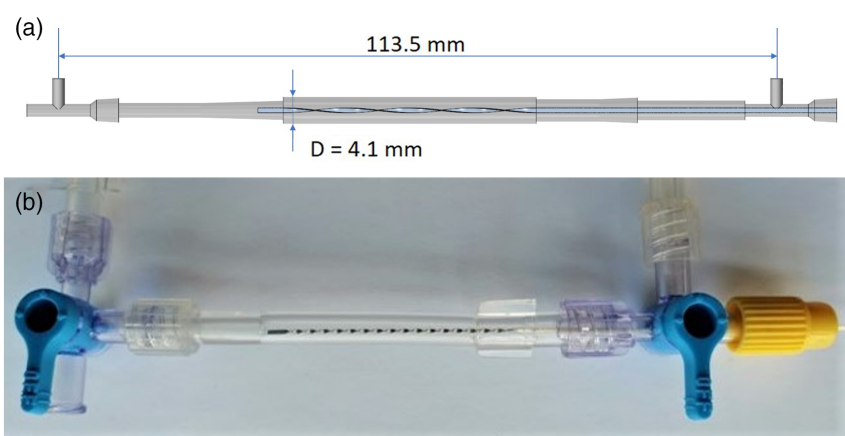


Figure 6. a) A CAD model of the internal dimensions of the test section and the cell probe provides the basis for the CFD simulations. b) A photo of a test section as it was used in the experiment. Flow direction is from left to right.

(1000 cells mL⁻¹). As soon as the BMProbes are in the system, the experiment is started, and the cell suspension is circulated with the roller pump. The flow rate can be precisely adjusted with the roller pump. It is calculated so that the mean flow velocity in the test section is the same as the desired velocity. After 60 min the probes are removed from the system, washed, and rehydrated for 5 min with PBS and then fixated with Acetone for 3 min. After further washing, the probes are stained with Hoechst fluorescent dye (1:10 000 in PBS). The deposited HUVECs are now visible under the fluorescence microscope and can be counted. To determine the positions of the attached cells on the probe, a photo is taken of every fourth winding on both sides of the probe (Figure 4b). In the current study, an Olympus BX51 microscope was used, to which an Axiocam 305 mono camera by Zeiss is attached. The images were processed by Zen 3.0 software.

Numerical Study: In order to simulate the flow around the BMProbe, the test section and the probe—shown in Figure 6—must be modeled on the computer. For this purpose, the test section and the BMProbe were recreated with the computer-aided design (CAD) program Solidworks 2018 (Version SP05, Dassault Systemes).

In order to imitate the flow properties of blood, a 10% dextran solution was chosen for the cell suspension. Dextran solution, like blood, is a non-Newtonian fluid with a shear-thinning behavior. In order to quantify the viscosity of the used Dextran solution, viscosity measurements were performed with the rotational viscometer Bohlin Gemini HR from Malvern Instruments (United Kingdom) at a temperature of 20 °C, which corresponds to the room temperature during the experiments. It was found that the dextran solution shows a shear thinning behavior, which can be described with a power law

$$\eta(\dot{\gamma}) = k\dot{\gamma}^{n-1} \quad (3)$$

where η is the dynamic viscosity, $\dot{\gamma}$ is the shear rate, k and n are constants. For this reason, a non-Newtonian generalized power law must be selected as the model for the dynamic viscosity in STAR-CCM+.

Table 2 shows all values required for the non-Newtonian generalized power law. The mesh for the CFD simulation was created with STAR-CCM+ (Siemens PLM Software, version 14.02.012). A polyhedral mesh was

Table 2. In the CFD simulation, the viscosity of the dextran solution used in the experiment must be accurately modeled. The measured viscosity behavior can be simulated with STAR-CCM+ using a non-Newtonian generalized power law model. All the factors required for this are listed in the table.

k —Consistency factor	0.005914
n —Power law exponent	0.4337
Yield stress threshold	0.0 Pa
Yielding viscosity	1.0 Pa s
Minimum viscosity limit	0.006 Pa s
Maximum viscosity limit	1.0 Pa s

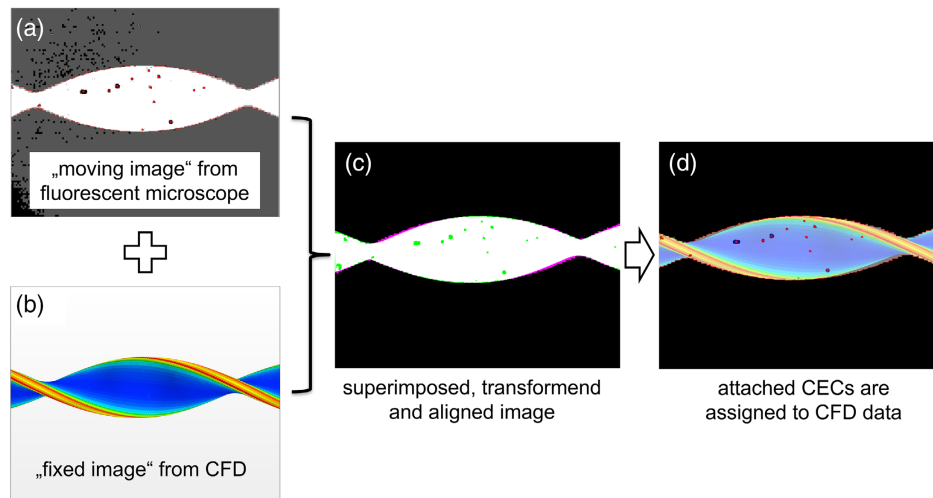


Figure 7. Workflow of the image registration, superimposition and transformation generating images combining results of in vitro experiments with results of flow simulations. a) A fluorescence microscope image and b) an image from the CFD simulation are superimposed. c) As the microscope images were not always taken in the ideal position, the two images still have to be aligned with each other. A similarity transformation algorithm is used for this purpose. The result can be seen in (d). Each attached CEC is marked with a red dot and assigned to the data from the CFD simulation.

selected. As the near-wall flow is of primary interest in this study, the mesh in the direct vicinity of the probe was finer resolved. Therefore, a boundary layer on the surface of the probe was created and the base size in the near wall flow area was reduced. A mesh independence study showed that a base size of 150 μm is enough to reliably resolve the investigated parameters. For the boundary layer on the cell probe, the base size was refined down to 45 μm .

CFD simulations were performed in STAR-CCM+ (Siemens PLM Software, version 14.02.012). A finite volume formulation is used to discretize the continuity equation for incompressible fluid and momentum equations. Stationary flow conditions are assumed. In order to classify the flow in the test section correctly and to select the correct physical models for the simulation, a Reynolds estimation was done. With a maximum Reynolds number of 210, a laminar and steady flow can be expected.

Postprocessing: The CFD investigation has shown that the near wall flow along the probe is identical for each winding. For this reason, it was possible to compare the CFD data from one winding segment with the experimental data from all windings of the probe.

Using a MATLAB program, the original microscope images were inverted and the contrasts were intensified. Afterward, the contour of the probe could be recognized and the position of the attached CECs could be determined with an edge detection algorithm (MATLAB *bwboundaries*, 2019).

Figure 7 shows the workflow of the image comparison. The inverted microscope image with the recognized edges of the probe and the attached cells (Figure 7a) and an image from the simulation from the same case (here $\nu = 2 \text{ cm s}^{-1}$, Figure 7b) form the baseline data of the method. Figure 7c shows the superimposition of both. They do not yet cover each other exactly. Therefore, an intensity-based image registration function is used to superimpose and align the two images. The image from the simulation always remains the “fixed image” and the microscope images becomes the “moving image” which is transformed with a similarity transformation consisting of translation, rotation, and scale (MATLAB *imregister*, 2019).

This transformation must be done for every microscope image because they are often slightly shifted or twisted. After the transformation, the position data of the attached CECs are saved in the coordinate system of the “fixed image.”

Figure 7d shows the transformed microscope image (red hull) aligned with the “fixed image” from the CFD simulation. The red dots mark the center of the attached CECs. Using a MATLAB program, it is possible

to assign the data from the CFD (e.g., WSR or WSR) to each of these attached cells.

The whole experiment was performed and evaluated with four different mean flow velocities. As the flow around the probe is the same for each winding, all images can be merged into one image for each velocity.

Acknowledgements

This study was supported by the Investitionsbank Berlin and the European Regional Development Fund (grant no. 10165865). Michael Lommel (Institute for Computer-assisted Cardiovascular Medicine, Charité – Universitätsmedizin Berlin) and Prof. Dr. Michael Gradzielski (Institute for Chemistry, Technische Universität Berlin) are thanked for conducting the rheological tests. Last but not least, the authors would like to thank the deceased Prof. Affeld for all his support, help, and inspiration.

Open access funding enabled and organized by Projekt DEAL.

Conflict of Interest

The authors declare no conflict of interest.

Data Availability Statement

The data that support the findings of this study are available from the corresponding author upon reasonable request.

Keywords

cell attachment, circulating endothelial cells, computational fluid dynamics, liquid biopsy

Received: October 27, 2021
Published online: January 13, 2022

- [1] WHO, *Global Health Estimates 2020: Deaths by Cause, Age, Sex, by Country and by Region, 2000–2019*, World Health Organization, Geneva **2020**.
- [2] A. D. Blann, A. Woywodt, F. Bertolini, T. M. Bull, J. P. Buyon, R. M. Clancy, M. Haubitz, R. P. Hebbel, G. Y. H. Lip, P. Mancuso, J. Sampol, A. Solovey, F. Dignat-george, *Thrombosis Haemostasis* **2005**, *3*, 228.
- [3] M. Farinacci, T. Krahn, W. Dinh, H.-d. V. Med, H.-d. D. J. Wagner, T. Konen, O. V. Ahsen, *Res. Pract. Thromb. Haemost.* **2019**, *3*, 49.
- [4] M. Wood, S. Damani, O. Libiger, S. Topol, P. Kuhn, K. Bethel, M. Connelly, C. Rao, R. Gollapudi, R. Goldberg, A. Bacconi, V. M. Fowler, N. J. Schork, R. Serry, S. Haaser, S. Knowlton, E. J. Topol, B. Carragher, J. Jiang, A. H. Chourasia, K. Rapeport, *Sci. Transl. Med.* **2012**, *4*, 126.
- [5] U. Erdbruegger, M. Haubitz, A. Woywodt, *Clin. Chim. Acta* **2006**, *373*, 17.
- [6] U. Erdbruegger, A. Dhaygude, M. Haubitz, A. Woywodt, *Curr. Stem Cell Res. Therapy* **2010**, *5*, 294.
- [7] S. J. Hao, Y. Wan, Y. Q. Xia, X. Zou, S. Y. Zheng, *Adv. Drug Delivery Rev.* **2018**, *125*, 3.
- [8] F. D. Scherag, R. Niestroj-Pahl, S. Krusekopf, K. Lücke, T. Brandstetter, J. Rühle, *Anal. Chem.* **2017**, *89*, 1846.
- [9] N. Saucedo-Zeni, S. Mewes, R. Niestroj, L. Gasiorowski, D. Murawa, P. Nowaczyk, T. Tomasi, E. Weber, G. Dworacki, N. G. Morgenthaler, H. Jansen, C. Propping, K. Sterzynska, W. Dyszkiewicz, M. Zabel, M. Kiechle, U. Reuning, M. Schmitt, K. Lücke, *Int. J. Oncol.* **2012**, *41*, 1241.
- [10] J. Swennenhuis, G. van Dalum, L. Zeune, L. Terstappen, *Expert Rev. Mol. Diagnostics* **2016**, *16*, 1291.
- [11] F. D. Scherag, T. Brandstetter, J. Rühle, *Biomicrofluidics* **2018**, *12*, 1.
- [12] L. Dizdar, G. Fluegen, G. Dalum, E. Honisch, R. P. Neves, H. Neubauer, T. Fehm, A. Rehders, A. Krieg, T. Wolfram, N. H. Stoecklein, *Mol. Oncol.* **2019**, *13*, 1548.
- [13] O. Hofmann, G. Voirin, P. Niedermann, A. Manz, *Anal. Chem.* **2002**, *74*, 5243.
- [14] T. David, S. Thomas, P. Walker, *Med. Eng. Phys.* **2001**, *23*, 299.
- [15] F. F. Weller, *J. Math. Biol.* **2008**, *57*, 333.
- [16] K. Affeld, J. Schaller, T. Wölken, T. Krabatsch, U. Kertzsch, *Biointerphases* **2016**, *11*, 029804.
- [17] N. S. Lynn, J. I. Martínez-López, M. Bocková, P. Adam, V. Coello, H. R. Siller, J. Homola, *Biosens. Bioelectron.* **2014**, *54*, 506.
- [18] N. Aristokleous, J. G. Houston, L. D. Browne, S. P. Broderick, E. Kokkalis, S. J. Gandy, M. T. Walsh, *Int. J. Numer. Methods Biomed. Eng.* **2018**, *34*, 11.
- [19] A. Zydney, C. Colton, *Int. J. Multiphase Flow* **1988**, *10*, 77.
- [20] S. Damani, A. Bacconi, O. Libiger, A. H. Chourasia, R. Serry, R. Gollapudi, R. Goldberg, K. Rapeport, S. Haaser, S. Topol, S. Knowlton, K. Bethel, P. Kuhn, M. Wood, B. Carragher, N. J. Schork, J. Jiang, C. Rao, M. Connelly, V. M. Fowler, E. J. Topol, *Sci. Transl. Med.* **2012**, *4*, 126.
- [21] K. Bethel, M. S. Luttgen, S. Damani, A. Kolatkar, R. Lamy, M. Sabouri-Ghomi, S. Topol, E. J. Topol, P. Kuhn, *Phys. Biol.* **2014**, *11*, 016002.
- [22] H.-J. Park, Y. Zhang, S. P. Georgescu, K. L. Johnson, D. Kong, J. B. Galper, *Stem Cell Rev.* **2006**, *2*, 93.